Mode-superposition-induced transparency

Rosenberger, A., Bui, Khoa

A. T. Rosenberger, Khoa V. Bui, "Mode-superposition-induced transparency," Proc. SPIE 12016, Optical and Quantum Sensing and Precision Metrology II, 120160Z (2 March 2022); doi: 10.1117/12.2617250

SPIE.

Event: SPIE OPTO, 2022, San Francisco, California, United States

Invited Paper

Mode-superposition-induced transparency

A. T. Rosenberger* and Khoa V. Bui
Department of Physics, Oklahoma State University, Stillwater, OK, USA 74078-3072

ABSTRACT

Induced transparency in a microresonator can result from cross-polarization coupling of two coresonant orthogonally polarized whispering-gallery modes of very different *Q*. The coupling creates supermodes that are superpositions of the two modes. Mode superpositions that result from simultaneous excitation of two orthogonally polarized modes can also show induced transparency, even in the absence of cross-polarization coupling. Induced transparency is accompanied by pulse delay, and it is also possible to observe induced attenuation with pulse advancement or delay. These effects are proposed theoretically, modeled numerically, and confirmed experimentally; a summary is presented here.

Keywords: microresonator, whispering-gallery modes, induced transparency

1. INTRODUCTION

Polarization effects in whispering-gallery-mode (WGM) microresonators represent a topic of increasing interest and importance.[1-6] We have previously studied coupled-mode-induced transparency (CMIT) and Autler-Townes splitting (ATS) with pulse delay, and coupled-mode-induced attenuation (CMIA) with pulse advancement or delay, when there is coupling between two coresonant modes with very different quality factors (*Q*s) and orthogonal polarizations.[7-9] These behaviors may be exploited for numerous applications such as signal processing and optical sensing.[10-12]

In our earlier work,[7-9] the mode coupling under study was cross-polarization coupling, resulting from the spin-orbit interaction of light in a microresonator's WGMs. The interaction between the spin and extrinsic orbital angular momentum of light in a WGM causes a weak polarization rotation, resulting in cross-polarization coupling (CPC). This is made possible by slight axial asymmetry of the resonator, for example, a hollow bottle resonator. The different axial extent of the coupled modes, one TE (transverse electric) and one TM (transverse magnetic), then results in their coupling being nonreciprocal.

If the CPC amplitudes are t_{21} for coupling from mode 1 (input) to mode 2 and $-t_{12}$ for 2 to 1 coupling (see Fig. 1), the destructive interference that gives CMIT comes from light coupled from 1 to 2 and back into 1, so that this contribution to the intracavity mode 1 field amplitude picks up a factor of $-T_c = -t_{21}t_{12}$, where T_c is the CPC strength. The mode coupling creates supermodes (analogous to the normal modes of coupled oscillators) that are linear superpositions of TE and TM.

The existence of these linear superpositions created by CPC led us to wonder what would happen in a system in which linear superpositions of coresonant TE and TM modes resulted from a process different from mode coupling. The resulting investigation is reported here. Again, the two modes will have very different *Q*s, but there is no CPC. The superposition is created by injecting light that is linearly polarized at 45°, simultaneously exciting both TE and TM. As in the CPC experiments, we detect the throughput light of the same polarization as the input, 45°. We find behavior qualitatively the same as in the CPC case, namely mode-superposition-induced transparency (MSIT) with pulse delay and mode-superposition-induced attenuation (MSIA) with pulse advancement or delay. (Since there is no mode coupling, there is no ATS.) In the CPC case, output is also observed on the polarization orthogonal to the input polarization; fitting this output to a model allows us to find the nonreciprocity in CPC, i.e., the ratio of amplitudes $b = t_{21}/t_{12}$, as discussed in another presentation in this conference (12016-60).[13] In the MSIT/MSIA case, output is also observed on the polarization orthogonal to the input, which in this case is at –45°. This indicates that there is now coupling between 45° and –45°. These effects are proposed theoretically, modeled numerically, and confirmed experimentally; a summary is presented here. We begin with the model including CPC and simplify to the case applicable to MSIT and MSIA.

*atr@okstate.edu; phone 1 405 744-6742; fax 1 405 744-6811; rosenberger.okstate.edu

Optical and Quantum Sensing and Precision Metrology II, edited by
Jacob Scheuer, Selim M. Shahriar, Proc. of SPIE Vol. 12016, 120160Z
 · 0277-786X · doi: 10.1117/12.2617250

2. MODEL AND THEORY

2.1. Ring cavity model and theory for CMIT

We use a ring cavity model as shown in Fig. 1. In In Fig. 1, the subscripts 1 and 2 refer to the two orthogonal polarizations. E_{fj} is the input amplitude of polarization j (only polarization 1 is input, so $E_{f2} = 0$), and

$$E_{rj} = r_j E_{fj} + it_j E_{sj}, \tag{1}$$

is the throughput amplitude of polarization j. E_{sj} is the intracavity mode amplitude just before output coupling, and the input/output coupling coefficient is it_j, with $r_j^2 = 1 - t_j^2 = 1 - T_j$. The input and output coupling coefficients are taken to be equal, as described in Ref. 8.

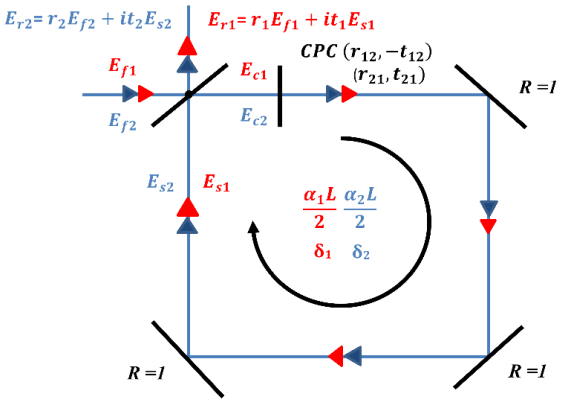

Fig. 1. Ring cavity model representing tapered-fiber coupling to a microresonator with intracavity cross-polarization coupling.

In Fig. 1, δ_j and $\alpha_j L$ are the round-trip phase (modulo 2π) and intrinsic loss for mode j; L is the resonator circumference. Cross-polarization coupling is represented in Fig. 1 as an effective intracavity wave plate and expressed by the coefficients t_{12} and t_{21}, where $t_{12}^2 = 1 - r_{12}^2$ and $t_{21}^2 = 1 - r_{21}^2$ are the polarization rotation probabilities per round trip, called T_s and T_p in Ref. 7.

The intracavity mode amplitudes E_{sj} satisfy the following time evolution equations:

$$\begin{aligned} \frac{d}{dt}E_{s1} &= -\gamma_1 E_{s1} - \frac{t_{12}}{\tau_{rt1}}E_{s2} + \frac{it_1}{\tau_{rt1}}E_{f1} - \frac{it_2 t_{12}}{\tau_{rt1}}E_{f2} \\ \frac{d}{dt}E_{s2} &= -\gamma_2 E_{s2} + \frac{t_{21}}{\tau_{rt2}}E_{s1} + \frac{it_2}{\tau_{rt2}}E_{f2} + \frac{it_1 t_{21}}{\tau_{rt2}}E_{f1} \end{aligned}, \tag{2}$$

With these and Eq. (1), the time evolution of the throughput amplitudes can be found. In Eqs. (2), $\tau_{rtj} = n_j L/c$ is the round-trip time for mode j, where n_j is the effective refractive index of the mode, and

$$\gamma_j = \frac{T_j + \alpha_j L}{2\tau_{rt_j}} - i\frac{\delta_j}{\tau_{rt_j}} = \kappa_j(1 + i\theta_j), \tag{3}$$

with $\kappa_j = \dfrac{\omega_0}{2Q_j}$ being the amplitude decay rate, or half the inverse of the photon lifetime in mode *j*, and θ_j being the offset of the resonant frequency of mode *j* (ω_0) from the input frequency in units of half the mode linewidth.

Equations (2) for the intracavity mode amplitudes are implicitly written in a frame rotating at ω_0. If this is not done, and if there is no input, so that γ_j becomes κ_j, the time evolution operator for the intracavity mode amplitude in the TM-TE (1-2) basis becomes

$$\begin{pmatrix} -i\omega_0 - \kappa_1 & -\gamma_{12} \\ \gamma_{21} & -i\omega_0 - \kappa_2 \end{pmatrix}, \tag{4}$$

where $\gamma_{12} = t_{12}/\tau_{rt1}$ and $\gamma_{21} = t_{21}/\tau_{rt2}$. This matrix has eigenvalues

$$\lambda_{\pm} = -i\omega_0 - \kappa_+ \pm \sqrt{\kappa_-^2 - \gamma_{21}\gamma_{12}}, \quad \text{where} \quad \kappa_{\pm} = \tfrac{1}{2}(\kappa_1 \pm \kappa_2). \tag{5}$$

These correspond to the two eigenvectors, which are the supermodes. If the radicand is positive, the supermodes have the same frequency but different decay rates, and the supermodes are linearly polarized superpositions of TM and TE – this is the case of CMIT; however, these superpositions are not simply symmetric and antisymmetric, and the polarizations of the supermodes are not, in general, orthogonal. When the CPC strength is increased enough to make the radicand negative, the supermode frequencies split and their polarizations become elliptical – this is the case of ATS. The point of transition, where the radicand is zero, is the exceptional point, where not only the two eigenvalues, but also the two eigenvectors, coalesce into a single eigenvalue and a single eigenvector.[14]

2.2. Model and theory for MSIT

For MSIT, the input light is linearly polarized at 45°, driving a superposition of E_{s1} and E_{s2} that we will call E_{s+}. We assume that there is no CPC, so the off-diagonal elements of the matrix of Eq. (4) are zero. That evolution matrix, in the basis that is the 1-2 basis rotated by 45°, then has the form

$$\begin{pmatrix} -i\omega_0 - \kappa_+ & -\kappa_- \\ -\kappa_- & -i\omega_0 - \kappa_+ \end{pmatrix}, \tag{6}$$

where the mode amplitudes forming the new basis are

$$E_{s\pm} = \tfrac{1}{\sqrt{2}}(E_{s1} \pm E_{s2}). \tag{7}$$

Now, even if there is no CPC between E_{s1} and E_{s2}, E_{s+} and E_{s-} will be coupled if $\kappa_- \neq 0$. Since, as in CMIT, we will assume that $Q_1 << Q_2$ or $\kappa_1 >> \kappa_2$, this will be the case and this coupling gives rise to MSIT. The eigenvalues of the matrix of Eq. (6) are

$$\lambda_{\pm} = -i\omega_0 - \kappa_+ \pm \kappa_-, \tag{8}$$

so there is no possibility of ATS; in fact, the supermodes are seen to be the original 1 and 2, i.e., TM and TE.

Taking the time derivative of Eq. (1) and using Eqs. (2), we can model the throughput response to an input pulse. By solving Eqs. (2) in steady state, we can model the throughput spectrum, IT being characterized by a dip with a central narrow spike and IA being characterized by a dip with a central narrower dip.[8] Now we can do the same for MSIT/MSIA. Let the input mode amplitude be E_{f+}, defined in terms of E_{f1} and E_{f2} as in Eq. (7), and similarly the throughput mode amplitude is E_{r+}, so that the input light is linearly polarized at 45°, and the throughput at 45° is detected. Set $t_{12} = t_{21} = 0$ in Eqs. (2) and find the relative throughput to be given by

$$\frac{E_{r+}}{E_{f+}} = \frac{1}{2}\left[\frac{\alpha_1 L - T_1 - i2\delta}{\alpha_1 L + T_1 - i2\delta} + \frac{\alpha_2 L - T_2 - i2\delta}{\alpha_2 L + T_2 - i2\delta}\right]. \tag{9}$$

An example of a simulated MSIT throughput spectrum (the squared modulus of the expression in Eq. (9)) is shown in Fig. 2, along with the simulated pulse response for the same parameter values. The width of the central spike (transparency

window) is approximately the same as the linewidth of the higher-Q mode 2, and the throughput pulse is seen to be delayed and reduced in amplitude compared to the input pulse.

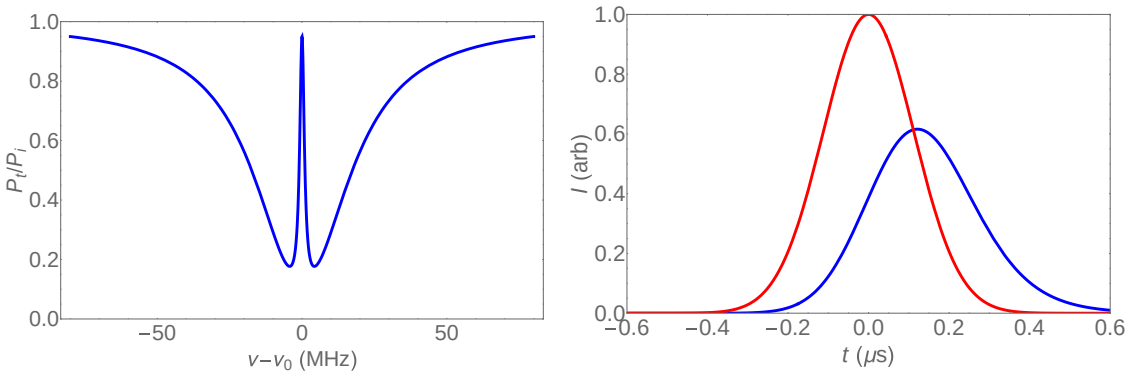

Fig. 2. Simulated MSIT throughput spectrum and delayed output pulse (blue) compared to the input pulse (red).

Write Eq. (9) in polar form, calling the phase ϕ; then the throughput delay τ of an input pulse can be found from

$$\tau = \frac{nL}{c}\left.\frac{d\phi}{d\delta}\right|_{\delta=0}. \tag{10}$$

(We will assume that modes 1 and 2 have the same effective index n and thus the same round-trip time.) As shown earlier,[15] the value of x_1x_2, where $x_j = T_j/\alpha_j L$, determines whether a pulse will be delayed or advanced. If $x_1x_2 > 1$, the pulse will be delayed; if $x_1x_2 < 1$, the pulse will be advanced.

To investigate the throughput spectrum, use Eq. (3) to write Eq. (9) as

$$\left|\frac{E_{r+}}{E_{f+}}\right| = \frac{1}{2}\left|\frac{\dfrac{1-x_1}{1+x_1}+i\theta_1}{1+i\theta_1} + \frac{\dfrac{1-x_2}{1+x_2}+i\theta_2}{1+i\theta_2}\right|. \tag{11}$$

What is measured will be the square of this, i.e., the ratio of throughput intensity or power to input intensity or power. Keep in mind that θ_j is the frequency detuning from resonance in units of the linewidth of mode j. Our condition that $Q_1 << Q_2$ means that mode 2 has a much narrower linewidth than mode 1. Thus it is possible to have a detuning such that $\theta_1 << 1 << \theta_2$. At this detuning, the throughput will be just outside the central spike or dip; comparing Eq. (11) evaluated at this detuning to its evaluation at zero detuning will determine whether we have MSIT (greater at zero) or MSIA (less at zero). At zero, $\theta_1 = \theta_2 = 0$, and

$$\left|\frac{E_{r+}}{E_{f+}}\right| = \frac{|1-x_1x_2|}{(1+x_1)(1+x_2)}, \tag{12}$$

whereas, when $\theta_1 << 1 << \theta_2$,

$$\left|\frac{E_{r+}}{E_{f+}}\right| = \frac{1}{1+x_1} = \frac{1+x_2}{(1+x_1)(1+x_2)}. \tag{13}$$

To have pulse advancement, the numerator of Eq. (12) will be $1-x_1x_2$, which can never be greater than $1+x_2$, so advancement is only possible in MSIA. For delay, the numerator is x_1x_2-1, which can be greater or less than $1+x_2$, so delay can occur in both MSIT and MSIA.

3. EXPERIMENTAL RESULTS

The experimental setup used is shown in Fig. 3. The tunable diode laser (1550 nm wavelength) is scanned in frequency and its free-space beam passes through an acousto-optic modulator. Wave plates and a compression-based polarization controller are used to control the input polarization. The coupling fiber is made adiabatically bi-tapered and brought into contact with the hollow-bottle resonator (HBR) in its equatorial plane using a 3D translation stage (not shown). The HBR is mounted on a piezo-controlled holder for strain tuning. The length of fiber after the HBR is kept short and straight to preserve the polarization.

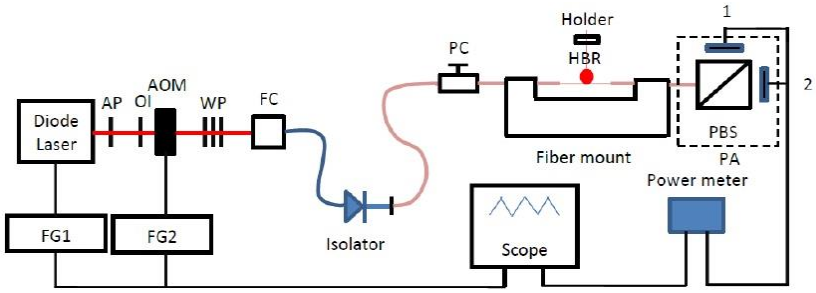

Fig. 3. Experimental setup.

In all cases, the resonator is kept inside an acrylic box to minimize temperature fluctuations and other effects of air movement. The output signal is sent to a polarization analyzer (PA), which includes a polarizing beam splitter (PBS) plus two detectors and can be rotated about the fiber axis so that either detector can detect either polarization. For data analysis, the detector signals are separately input to the oscilloscope.

Light polarized at 45° in the TM-TE basis is input, and the HBR is strain-tuned to TE-TM coresonance, and the throughput spectrum of the input polarization (the PA is rotated about the fiber axis by 45° from the orientation shown in Fig. 3) is observed. An MSIT or MSIA feature is observed when the laser is scanned; for the pulse response, the laser is tuned to resonance. Individual mode parameters are measured by tuning away from coresonance and using input of the two polarizations sequentially. Those parameters are, for mode j: quality factor Q_j, relative throughput dip depth M_j, and the coupling regime (overcoupled means $x_j > 1$ and undercoupled means $x_j < 1$). In addition, the mistuning from coresonance and the detuning of the pulse center frequency from resonance are estimated. Using those parameters, the model is fitted to the experimental spectral trace. Figure 4 shows an example.

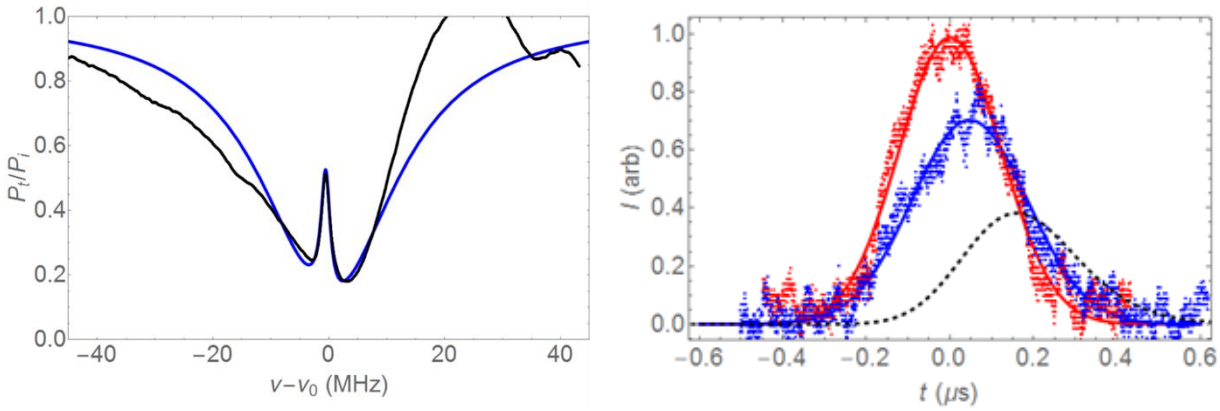

Fig. 4. MSIT with 170-μm-radius HBR. Left: Experimental (black) and model (blue) throughput spectra. Right: Experimental input (red) and throughput (blue) pulses, with an input pulse width of 285 ns and a delay of 47 ns, and model throughput pulse (dashed black), with a delay of 150 ns. Parameter values: $M_1 = 0.61$ (overcoupled), $M_2 = 0.32$ (overcoupled), $Q_1 = 6.9\times10^6$, $Q_2 = 1\times10^8$; mistuning of mode 2 resonance from mode 1 resonance = -0.5 MHz, pulse detuning = -0.5 MHz.

4. DISCUSSION

Superposition of uncoupled WGMs of orthogonal polarizations and very different *Q*s is studied theoretically and modeled numerically. The results of this analysis show that it is possible for the throughput to show MSIT, with pulse delay, and MSIA, with pulse advancement or delay. Experimental investigation confirms these results; MSIT with pulse delay has been observed, as in Fig. 4, and MSIA with pulse advancement and MSIA with pulse delay have also both been observed. Comparison of experimental results to the model predictions given the experimental parameter values shows qualitative agreement. Reasonable fits to the experimental throughput spectra are found, but the experimental and modeled amplitude and delay (or advancement) of the throughput pulse differ quantitatively, as illustrated in Fig. 4.

The most likely cause of the quantitative, but not qualitative, disagreement between experiment and model is mode overlap. Since the input light has both TE and TM components, modes of both polarization families are being excited. This makes it more difficult to achieve coresonance between a well-isolated TE WGM and a well-isolated TM WGM. It is easier in CMIT, when the input is of a single polarization.[8,9] Mode overlap can be reduced by using an HBR with a slightly different bulge profile, and carefully positioning a somewhat thicker tapered fiber with respect to it.

Preliminary investigations suggest that MSIT could provide a sensitivity enhancement over CMIT if used for dissipative sensing. With the analyte inside the HBR, only the WGM with the higher radial order might interact with it, if the lower-radial-order WGM does not have an internal fraction. This can change the shape of the throughput spectrum, in particular the height of the central spike. In general, any application for which induced transparency (or attenuation) is suited could potentially benefit from using MSIT rather than CMIT, since CPC is not required.

REFERENCES

[1] Konishi, H., Fujiwara, H., Takeuchi, S., and Sasaki, K., "Polarization-discriminated spectra of a fiber-microsphere system," Appl. Phys. Lett. 89, 121107 (2006).

[2] Ramelow, S., Farsi, A., Clemmen, S., Levy, J. S., Johnson, A. R., Okawachi, Y., Lamont, M. R. E., Lipson, M., and Gaeta, A. L., "Strong polarization mode coupling in microresonators," Opt. Lett. 39, 5134-5137 (2014).

[3] Liu, Y. C., Li, B.-B., and Xiao, Y.-F., "Electromagnetically induced transparency in optical microcavities," Nanophotonics 6, 789-811 (2017).

[4] Nasir, M. N. M., Gorajoobi, S. B., Murugan, G. S., and Zervas, M. N., "Polarization effects in optical microresonators," J. Opt. Soc. Am. B 36, 705-716 (2019).

[5] Kreismann, J., and Hentschel, M., "Spin-orbit interaction of light in three-dimensional microcavities," Phys. Rev. A 102, 043524 (2020).

[6] Wang, C., Jiang, X., Sweeney, W. R., Hsu, C. W., Liu, Y., Zhao, G., Peng, B., Zhang, M., Jiang, L., Stone, A. D., and Yang, L., "Induced transparency by interference or polarization," Proc. Natl. Acad. Sci. USA 118, e2012982118 (2021).

[7] Rosenberger, A. T., Dale, E. B., Bui, K. V., Gonzales, E. K., Ganta, D., Ke, L., and Rajagopal, S. R., "Cross-polarization coupling of whispering-gallery modes due to the spin-orbit interaction of light," Opt. Lett., 44, 4163-4166 (2019).

[8] Bui, K. V., and Rosenberger, A. T., "Coupled-mode-induced transparency and attenuation resulting from cross-polarization coupling," Phys. Rev. A 101, 033836 (2020).

[9] Ke, L., Rajagopal, S. R., and Rosenberger, A. T., "Dynamical determination of the strength of cross-polarization coupling in a whispering-gallery microresonator," Phys. Rev. A. 104, 053534 (2021).

[10] Foreman, M. R., Swaim, J. D., and Vollmer, F., "Whispering gallery mode sensors," Adv. Opt. Photon. 7, 168-240 (2015).

[11] Yoshiki, W., Honda, Y., Tetsumoto, T., Furusawa, K., Sekine, N., and Tanabe, T., "All-optical tunable buffering with coupled ultra-high *Q* whispering gallery mode microcavities," Sci. Rep. 7, 10688 (2017).

[12] Smith, D. D., Chang, H., Myneni, K., and Rosenberger, A. T., "Fast-light enhancement of an optical cavity by polarization mode coupling," Phys. Rev. A 89, 053804 (2014).

[13] Sandoval, K., Junaid Ul Haq, M., and Rosenberger, A. T., "Asymmetric cross-polarization coupling between microresonator whispering-gallery modes," Proc. SPIE 12016, to be published.

[14] Miri, M.-A., and Alù, A., "Exceptional points in optics and photonics," Science 363, eaar7709 (2019).

[15] Rosenberger, A. T., "Comparison of methods for achieving induced transparency or absorption with pulse delay or advancement in a single microresonator," Proc. SPIE 9763, 97631E (2016).